Electronic Journal of Biotechnology 74 (2025) 11–18

Contents lists available at ScienceDirect

Electronic Journal of Biotechnology

journal homepage: www.elsevier.com/locate/ejbt

Research article

Whole-transcriptome analysis reveals the characteristics of intramuscular fat circRNA expression and its associated network in grazing yaks of different months of age under cold stress ☆

Yaqian Liu, Yonggang Sun *, Yincang Han, Weiqin Ding, Shengwei Jin, Jianyu Chen, Fajie Gou

Academy of Animal Husbandry and Veterinary Sciences, Qinghai University, Xining, China
Qinghai Key Laboratory of Plateau Livestock Genetic Resources Protection and Innovative Utilization, Xining, China

GRAPHICAL ABSTRACT

Whole-transcriptome analysis reveals the characteristics of intramuscular fat circRNA expression and its associated network in grazing yaks of different months of age under cold stress

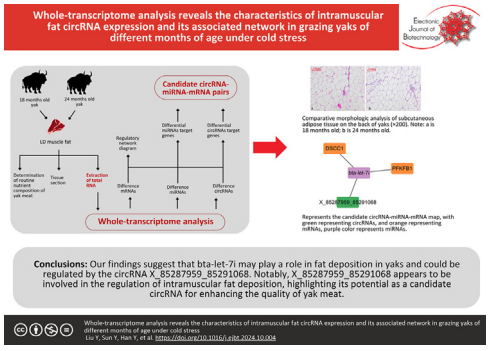

ARTICLE INFO

Article history:
Received 14 August 2024
Accepted 29 October 2024
Available online 9 January 2025

Keywords:
bta-let-7i
ceRNA
circRNA
Cold stress
Gene expression
Intramuscular fat
Meat quality
miRNAs
Whole-transcriptome

ABSTRACT

Background: The aim of this study was to screen circRNAs related to fat deposition in yaks, and to identify candidate circRNAs for yak meat quality improvement. Six male yaks with insignificant differences in body weights were selected as test subjects, and 3 yaks (G18_IMF) were randomly slaughtered at the beginning of the experiment, while the remaining 3 yaks were naturally grazed until 24 months of age (G24_IMF), and then slaughtered at the end of the experiment, and the intramuscular fat was collected from the dorsal muscle. At the end of the experiment, the yaks were slaughtered and the intramuscular fat from the back was collected for whole transcriptome sequencing.
Results: The results showed that 352 differential circRNAs, 86 differential miRNAs and 3981 differential mRNAs were found. miRNAs and mRNAs network regulation maps were successfully constructed through gene expression correlation analysis and target gene prediction.
Conclusions: Taking the intersection of the predicted circRNA target genes with the differential miRNAs for intramuscular fat in yaks of different months of age, we obtained two candidate ceRNA pairs that might be related to intramuscular fat deposition in yaks, and found that bta-let-7i might be related to fat deposition in yaks and might be regulated by X_85287959_85291068, and that

☆ Audio abstract available in Supplementary material.

Peer review under responsibility of Pontificia Universidad Católica de Valparaíso

* Corresponding author.
E-mail address: sunyg410@163.com (Y. Sun).

https://doi.org/10.1016/j.ejbt.2024.10.004

Yaks

X_85287959_85291068 could be a candidate circRNA to enhance the quality of yak meat. The results may provide a reference for further investigation of the regulatory network of intramuscular fat deposition in yak.

How to cite: Liu Y, Sun Y, Han Y, et al. Whole-transcriptome analysis reveals the characteristics of intramuscular fat circRNA expression and its associated network in grazing yaks of different months of age under cold stress. Electron J Biotechnol 2025;74. https://doi.org/10.1016/j.ejbt.2024.10.004.

1. Introduction

As the "boat of the snowy region", yaks are mainly distributed in the high-altitude areas of 3000 m ~ 5000 m on and around the Tibetan Plateau [1], providing herders with meat, milk, wool and other necessities, as well as having a high economic value. Accompanied by the gradual improvement of people's living standard, the requirements for meat quality are getting higher and higher [2]. Yak meat is characterized by low fat, high protein, rich in a variety of fatty acids and amino acids, etc. However, the intramuscular fat (IMF) content in yak meat is low, which seriously affects the taste and flavor of yak meat. IMF is formed due to a large accumulation of intramuscular fat, and the tenderness, flavor and quality of meat are affected by IMF and fatty acids, among others [3,4]. Therefore, it is important to investigate the deposition pattern of intramuscular fat for yak meat quality improvement as well as for the improvement of local herders' living standard. The aim of this study was to compare the changing patterns of IMF in yaks of different months of age during the cold season, to sequence the whole transcriptome of IMF in yaks of different months of age, to compare the expression of circRNAs, miRNAs and mRNAs differing in intramuscular fat in yaks of different months of age, and to screen for candidate circRNA-miRNA-mRNA pairs that regulate intramuscular fat in yaks in an attempt to investigate the changing patterns of circRNAs in intramuscular fat of yaks and to lay the foundation for further research on the mechanism of action of intramuscular fat deposition.

2. Material and methods

2.1. Experimental materials and feeding management

Six male yaks of 18 months of age with good growth condition and insignificant differences in intramuscular fat were provided by Meilongpal Livestock Management Specialized Cooperative in Qilian County, Qinghai Province (mean elevation 3169 m). At the beginning of the experiment (October), three yaks (G18_IMF) were randomly selected for slaughter, and the remaining three yaks (G24_IMF) continued to graze naturally until 24 months of age. Table S1 indicates the forage nutrient levels. They were slaughtered at the end of the experiment, and the fat on their backs was collected, put into a liquid nitrogen tank and transported back to the laboratory, where it was stored at −80°C for spare use. Approximately, 500 g of longissimus dorsi muscle (LD) samples was collected after slaughter, stored in a sealed thermostat (0–4°C), and then transported back to the laboratory for storage at −20°C to measure their nutritional quality. Dorsal surface fat, which is physiologically similar to intramuscular fat and is easier to collect [5], was taken and placed in a fixative for tissue sectioning. Fig. 1 shows the flow chart of the experiment.

2.2. Determination of routine nutrient composition of yak meat

According to (GB/T 5009.5-2003) semi-micro Kjeldahl method for the determination of crude protein, according to (GB/T 5009.4-2010) method for the determination of crude ash, according to (GB/T 5009.3-2010) direct drying method for the determination of moisture, according to (GB/T 5009.6-2010) Soxhlet extraction method for the determination of crude fat.

2.3. RNA extraction, library preparation and sequencing

Total RNA was extracted from the tissue using TRIzol® Reagent according to the manufacturer's instructions. Then, RNA quality was determined by 5300 Bioanalyser (Agilent) and quantified using the ND-2000 (NanoDrop Technologies). Only high-quality RNA sample (OD260/280 = 1.8 ~ 2.2, OD260/230 ≥ 2.0, RIN ≥ 6.5, 28S:18S ≥ 1.0, > 1 μg) was used to construct sequencing library. Small RNA libraries were generated using QIAseq miRNA Library Kit (Qiagen) following the manufacturer's recommendations, and mRNA + lncNRA + circRNA libraries were generated by Illumina Stranded Total RNA Prep, Ligation with Ribo-Zero Plus. They were then sequenced using an Illumina NovaSeq 6000 by Shanghai Majorbio Bio-pharm Biotechnology Co., Ltd. (Shanghai, China).

2.4. Identification of circRNAs

After the clean reads were aligned to the reference genome, junctions of the unmapped reads were identified using a back-splice algorithm. CIRI2 and Findcirc were used to predict circRNAs. The expression levels of circRNAs were reflected by the number of mapped back-splicing junction reads per million mapped reads (RPM). The analysis was performed using DEGseq (version 1.30.0) software, with a screening threshold of |log2FC| ≥ 1.000, padjust < 0.001.

2.5. Identification of small RNAs

Firstly, all clean mapped tags were aligned with miRNAs in the miRBase22.0 database (https://www.mirbase.org/) to got known miRNA. Then, the rest of the tags were aligned with Rfam database and Repbase database to remove ribosomal RNA (rRNA), transfer RNA (tRNA), small nuclear RNA (snRNA), small nucleolar RNA (snoRNA) and other ncRNA and repeats. Next, the unannotated tags were predicted to be and identified as novel miRNAs using miRdeep2 software, according to the tag positions in the genome and their hairpin structures.

2.6. Prediction of miRNA target genes

miRanda for animal was used to predict miRNA targets.

2.7. Identification of differentially expressed RNAs

The "DESeq2" package in R software was applied to screen DEcircRNAs, DEmRNAs and DEmiRNAs. We identified the significant DEcircRNAs and DEmiRNAs in comparable group (p < 0.05 and |Log2FC| > 1). The thresholds of |LogFC| > 1 and pdjust < 0.05 were used to screen the significant DEmRNAs. Gene Ontology (GO) term

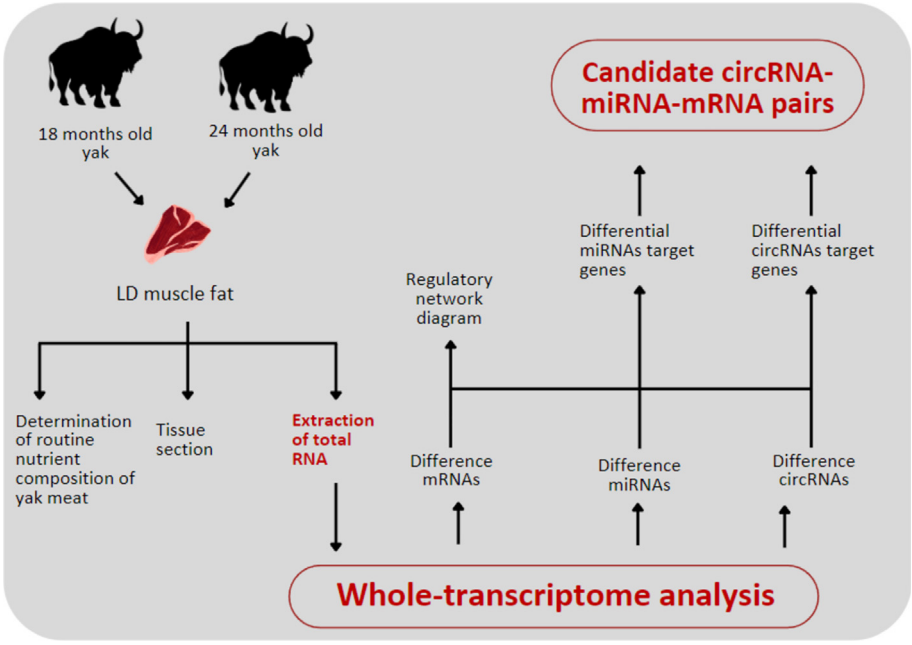

Fig. 1. Experimental flow chart.

and the Kyoto Encyclopedia of Genes and Genomes (KEGG) functional enrichment analysis were performed for DEmiRNAs (using the DEmiRNA target genes), and DEmRNAs using the Goatools (version 0.6.5) and KOBAS (version 2.1.1) tool with the BH method corrected for *p*-values by default, and when the corrected *p*-value (Padjust) < 0.05, it was considered that there was a significant enrichment for this function, respectively. Finally, candidate circRNA-miRNA-mRNA pairs that regulate fat deposition were screened. The experimental flow is shown in Fig. 1.

2.8. qRT-PCR validation

The accuracy of the sequencing results was verified by qRT-PCR. 3 miRNAs, 3 RNAs and 3 circRNAs were randomly selected. qRT-PCR was carried out using SYBR Green Dye Fluorescence Quantification Kit. The primers were designed with reference to the relevant gene sequences of bovine (*Bos taurus*) in NCBI, and GAPDH was used as the internal reference gene for circRNA and mRNA, and U6 was used as the internal reference gene for miRNA, the primers were designed using Primer 5.0 software and sent to Sangon Biotech Ltd. for synthesizing (Table S2).

3. Results

3.1. Comparison of conventional nutrients

The crude fat content in the LD of 18-month-old yaks was significantly higher than that of 24-month-old yaks ($p < 0.05$). There were no significant differences in ash and crude protein contents ($p > 0.05$) (Table 1).

3.2. Effect of cold season stress on the morphology of back adipose tissue in yak

As shown in Table 2 and Fig. 2, the length diameter of fat cells on the back of 18-month-old yaks was significantly higher than that of 24-month-old yaks ($p < 0.05$); the density of fat cells in 18-month-old yaks was highly significantly lower than that of 24-month-old yaks ($p < 0.01$).

3.3. Sequencing data quality control

In this study, a total of six sequencing libraries were constructed, and the dorsal intramuscular fat libraries of 18-month-old yak (yak_18m_G_IMF) and 24-month-old yak (yak_24m_G_IMF) were sequenced by Illumina platform. In the six sequencing libraries, the Error rate was controlled below 0.025%, the GC content was in the range of 45.8~51.34%, and the Q20 and Q30 of the six sequencing libraries were above 98.1% and 94.3%, respectively. The statistics of sequencing quality data are shown in Table S3. From the above results, it can be seen that the quality of sequencing data is good, which meets the requirements of subsequent experiments.

3.4. Differential mRNA screening and pathway enrichment analysis

As shown in Fig. 3a, by mRNA sequencing of yak intramuscular adipose tissue, there were 24,089 mRNAs in G24_IMF, 23,987 mRNAs in G18_IMF, and 22,112 mRNAs were co-expressed in G24_IMF and G18_IMF. As shown in Fig. 3d, **3981 G24**_IMF and

Table 1
Comparative analysis of conventional nutrient composition of yak meat.

Item	Part	18 months old	24 months old
Moisture (%)	LD	76.99 ± 0.11[a]	75.64 ± 0.74[ab]
Crude protein (%)	LD	23.02 ± 1.26	22.69 ± 2.78
Crude fat (%)	LD	3.20 ± 0.32[ab]	2.10 ± 0.09[b]
Ash (%)	LD	1.95 ± 0.19	2.07 ± 0.21

Note: Differences in lower case letters indicate significant differences ($p < 0.05$).

Table 2
Comparative analysis of various parameters of yak back adipocytes.

Items	18 months old	24 months old
Fat cells length and diameter (μm)	69.44 ± 3.94a	64.62 ± 8.10b
Fat cells are short in diameter (μm)	55.37 ± 1.07	51.65 ± 3.46
Mean diameter of fat cells (μm)	62.41 ± 8.13	58.14 ± 9.03
Fat cells density (N/mm2)	603.67 ± 16.80b	689.67 ± 40.05a

Note: Differences in lower case letters indicate significant differences ($p < 0.05$).

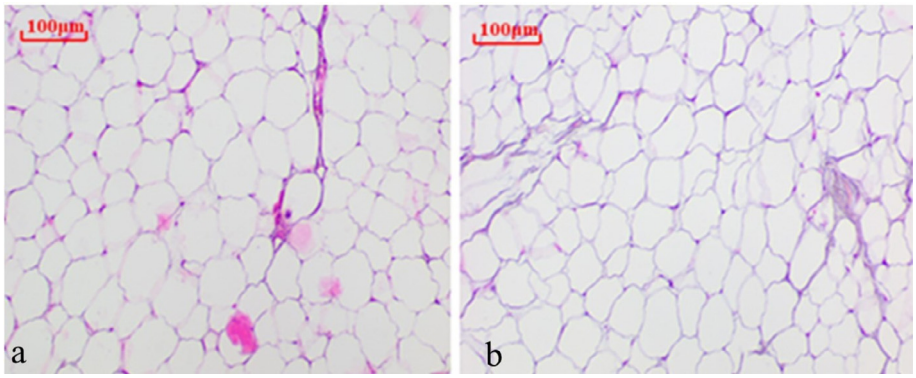

Fig. 2. Comparative morphologic analysis of subcutaneous adipose tissue on the back of yaks (×200). (a) corresponds to 18 months old; (b) corresponds to 24 months old.

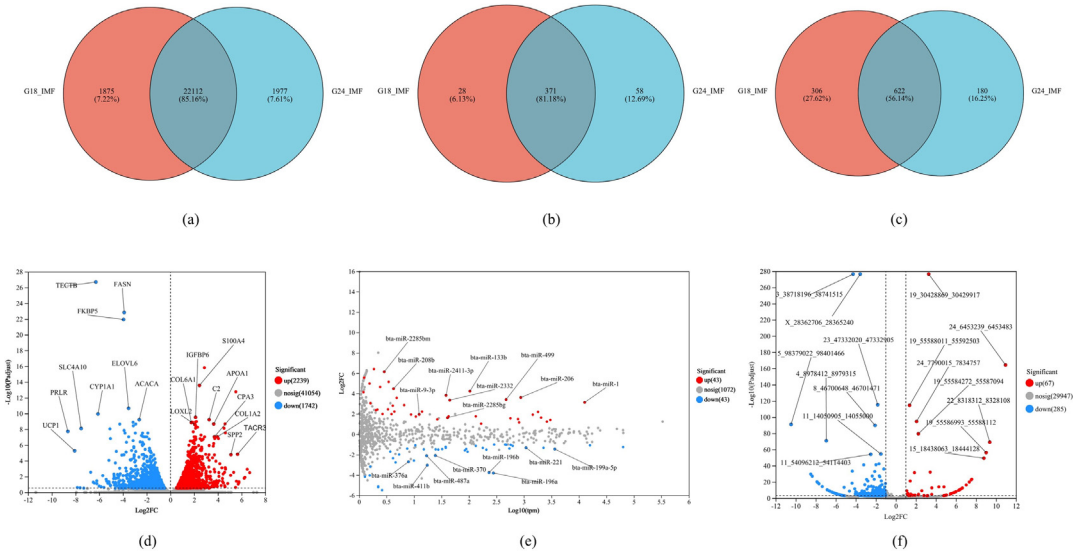

Fig. 3. Analysis of differential mRNAs, miRNAs and circRNAs. (a) Venn diagram between mRNA samples; (b) Venn diagram between miRNA samples; (c) Venn diagram between circRNA samples; (d) volcano plot of mRNA expression differences; (e) miRNA expression difference MA figure; (f) volcano plot of circRNA expression differences.

G18_IMF differential mRNAs were identified, of which 2239 were up-regulated and 1742 were down-regulated. The KEGG pathway enrichment map of differential mRNAs related to fat metabolism is shown in Fig. 4a.

3.5. Differential miRNA screening and pathway enrichment analysis

As shown in Fig. 3b, by miRNA sequencing of yak intramuscular adipose tissue, there were 429 miRNAs in G24_IMF and 399 miRNAs in G18_IMF; 371 miRNAs were co-expressed in G24_IMF and G18_IMF.

As in Fig. 3e, each point in the graph represents a specific miRNA, and by default, the red points indicate significantly up-regulated miRNAs, the blue points indicate significantly down-regulated miRNAs, and the gray points are non-significantly differentiated miRNAs. Eighty-six different miRNAs were identified between G24_IMF and G18_IMF, of which 43 were up-regulated and 43 were down-regulated.

3.6. Differential circRNA screening and pathway enrichment analysis

As shown in Fig. 3c, by circRNA sequencing of yak intramuscular adipose tissue, there were 802 circRNAs in G24_IMF, 928 circRNAs in G18_IMF, and 622 circRNAs were co-expressed in G24_IMF and G18_IMF.

As in Fig. 3f**, 352** differentiated circRNAs between G24_IMF and G18_IMF, of which 67 were up-regulated and 285 were down-regulated.

3.7. Target gene prediction

As shown in Table 3, miRanda software was used to predict the targeting relationships of differentially expressed circRNAs and mRNAs with differentially expressed miRNAs. It was found that 1 circRNA had 1 targeting relationship pair with 1 miRNA; 86 miRNAs had 1183 targeting relationship pairs with 918 mRNAs. Pathway enrichment analysis was performed on the target genes, and Fig. 4b shows the KEGG-enriched pathway associated with lipid metabolism, and pathway enrichment is tabulated in Table S4.

3.8. Construction of ceRNA network diagrams

The differentially expressed circRNA, miRNA and mRNA sequences were analyzed to find miRNAs with binding sites on circRNAs and mRNAs, which were visualized using Cytoscape software, and finally, the circRNA-associated ceRNA network was

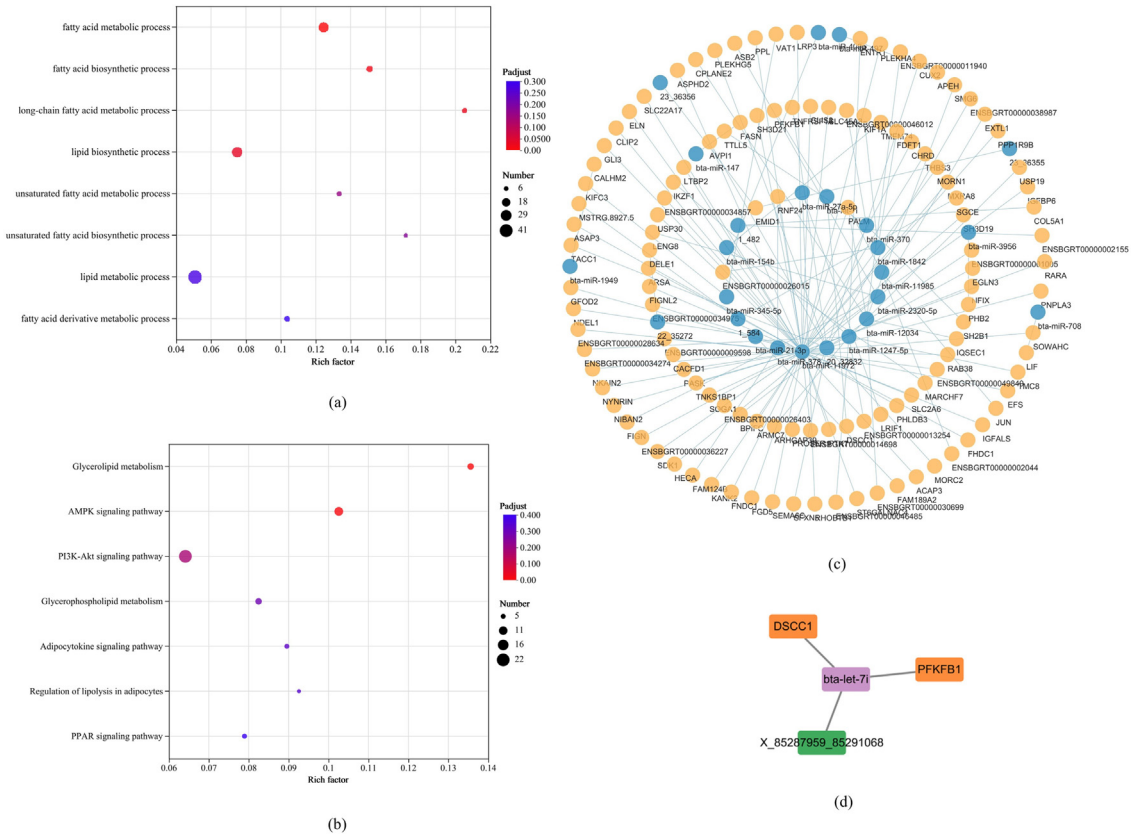

Fig. 4. KEGG enrichment pathway and network regulation map. (a) KEGG pathway enrichment map of differential mRNAs associated with fat metabolism; (b) KEGG pathway enrichment map of target genes associated with fat metabolism; (c) miRAN vs. mRNA regulatory network map, with blue representing mRNAs, and orange representing miRNAs; (d) Candidate circRNA-miRNA-mRNA map, with green representing circRNAs, and orange representing mRNAs, purple color represents miRNAs. (For interpretation of the references to color in this figure legend, the reader is referred to the web version of this article.)

Table 3
Target gene prediction (top 20).

miRNA name	Target transcript id	Target RNA type	target gene id	target gene name
bta-let-7i	X_85287959_85291068	circRNA	ENSBGRG00000025136	PIN4
bta-miR-21-3p	ENSBGRT00000001830	mRNA	ENSBGRG00000000954	FAM189A2
bta-miR-1247-5p	ENSBGRT00000024299	mRNA	ENSBGRG00000012869	EYA1
bta-miR-2320-5p	ENSBGRT00000013524	mRNA	ENSBGRG00000007378	
bta-miR-150	ENSBGRT00000047860	mRNA	ENSBGRG00000025875	
bta-miR-11985	ENSBGRT00000046904	mRNA	ENSBGRG00000025378	FAAP100
bta-miR-11972	ENSBGRT00000013571	mRNA	ENSBGRG00000007389	PIGU
bta-miR-133a	ENSBGRT00000020192	mRNA	ENSBGRG00000010838	SNCAIP
bta-miR-11972	ENSBGRT00000013789	mRNA	ENSBGRG00000007457	METTL21A
bta-miR-21-3p	ENSBGRT00000046906	mRNA	ENSBGRG00000021276	

constructed. The results showed that 25 miRNAs had binding sites with 133 mRNAs, and no circRNAs were found to have binding sites on miRNAs. The network relationship diagram is shown in Fig. 4c.

The predicted target gene bta-let-7i of circRNA: X_85287959_85291068 was taken to intersect with the differential miRNA target genes to obtain 2 pairs of candidate circRNA-miRNA-mRNA pairs that may regulate intramuscular fat in yak, as shown in Table 4 and visualized using Cytoscape software, as shown in Fig. 4d.

3.9. qRT-PCR validation

The results of the qRT-PCR verification of the differentially expressed genes are shown in Fig. 5**.** The transcriptome sequencing results of the differentially expressed genes are presented in Fig. S1. qRT-PCR was consistent with the transcriptome sequencing results.

4. Discussion

Yak is an ancient and primitive species of cattle, present in and around the Tibetan Plateau, and in small numbers in Mongolia,

Table 4
Candidate circRNA-miRNA-mRNA pairs.

circRNA	miRNA	mRNA ID	mRNA name
X_85287959_85291068	bta-let-7i	ENSBGRG00000015766	DSCC1
X_85287959_85291068	bta-let-7i	ENSBGRG00000007193	PFKFB1

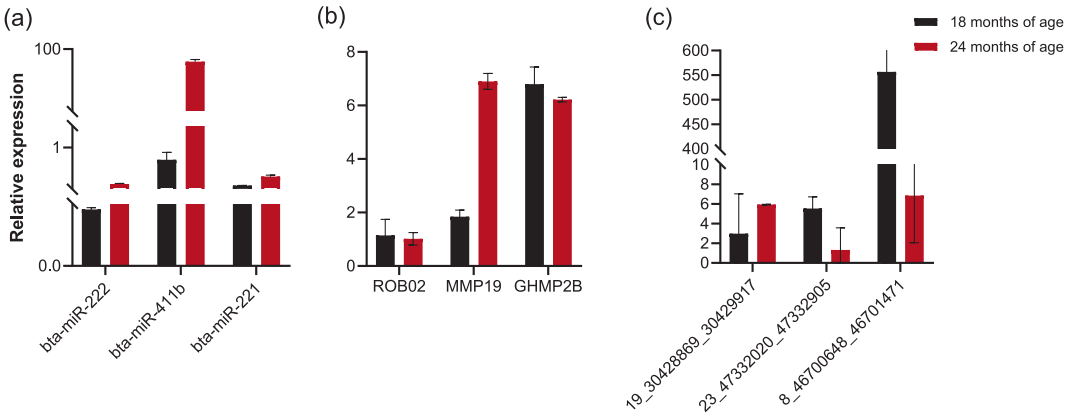

Fig. 5. Differently expressed gene validation results.

Bhutan, Russia, and India, and is a means of production and livelihood for plateau herders [6]. Fat deposition in animals is influenced by a combination of nerves, body fluids, hormones and fat-metabolizing enzymes [7,8]. For a long time, yak production has been mainly based on traditional grazing, so the nutritional value and quantity of pasture directly affect the growth performance of yaks. The fat deposition capacity of yaks varies with seasons and pastures, as "spring is weak, summer is strong, autumn is fat, and winter is aura" throughout the growth period of yaks. The crude fat content of the longest dorsal muscle of 18-month-old yaks was significantly higher than that of 24-month-old yaks ($p < 0.05$), which was attributed to the fact that yaks experienced a large amount of fat consumption during the cold season, resulting in the crude fat content of 18-month-old yaks being higher than that of 24-month-old yaks. At the end of the cold season, yaks can lose up to 25% of their body weight. Therefore, it is of great significance to investigate the intramuscular fat deposition pattern of yaks to promote the economic development of the plateau.

The closed ncRNA formed by reverse shearing of mRNA is circular RNA (circRNA), which is mainly found in the cytoplasm [9] and is highly resistant to ribonucleases. CircRNAs have a variety of biological functions such as competitive binding of miRNAs, regulating gene expression and encoding proteins [10]; at the same time, circRNAs are involved in the splicing of target genes and translation of genes into proteins, and studies have shown that circRNAs undergo a rolling cycle of amplification, which results in productivity that is 100-fold higher than that of linear transcripts [11]; circRNAs can also bind to host gene loci to form R-loops leading to pauses in gene transcription [12,13]; RNA-binding proteins bind to circRNAs to become scaffolds, decoys, and recruiters of proteins, binding to proteins and consolidating protein–protein interactions [14]. It has been reported that circRNAs can act as sponges to competitively bind miRNAs and participate in cell proliferation, apoptosis, differentiation, and other functions [15]. circRNAs can function as competing endogenous RNA (ceRNA) and participate in adipocyte regulatory processes [16,17,18,19]. It was found that circfut 10 inhibits peroxisome proliferator-activated receptor γ coactivator 1β by binding to let 7c thereby promoting bovine adipocyte proliferation and inhibiting adipocyte differentiation [20]; inhibition of circ-PLXNA1 expression increases the expression of duck adipose precursor cytokine 1, inhibits the expression of C/EBPα and FAS genes, and thereby reduces the ability of adipocyte differentiation [21]; circ PPARA can adsorb miR-429 and miR-200, which in turn affects porcine intramuscular adipogenesis [22]; circPPAR2 can adsorb miR-2366 to increase GK expression, which promotes porcine precursor adipocyte differentiation [23]. These studies suggest that circRNAs may play an important role in adipogenesis through the circRNA-miRNA-mRNA regulatory network. In order to investigate the role of circRNAs in the process of intramuscular fat deposition in yaks, this study utilized whole transcriptome sequencing technology to investigate the expression of circRNAs in intramuscular fat of yaks of different months of age. The results showed that a total of 352 differential circRNAs, 86 differential miRNAs and 3981 differential mRNAs were detected. So far, it is difficult to screen circRNAs related to fat deposition by the function of circRNAs. Therefore, in this study, we took the intersection of the target genes of differential circRNAs with the target genes of differential miRNAs and obtained 2 pairs of candidate circRNA-miRNA-mRNA pairs that may be related to intramuscular fat deposition in yak, which are: X_85287959_85291068-bta-let-7i-DSCC1 and X_85287959_85291068-bta-let-7i-PFKFB1. In this study, we found that the gene loci of PFKFB1 and DSCC1 were located near the X_85287959_85291068 transcriptional site, and that X_85287959_85291068 and bta-let-7i might regulate fat deposition in yak, but the specific function of the above ceRNA relationship pairs in intramuscular fat of yak still needs to be verified by further experiments. Lethal-7 (let-7) is the second miRNA to be discovered, and 17 members of the let-7 family have been identified, and the seed regions of each member are conserved in sequence and function across multiple tissues in multiple species [24]. let-7 was first found to regulate cell division in nematode worms, and further studies have revealed that let-7 also has a role in regulating organ development in animals. Johnson et al. [25] found that overexpression of let-7 in lung cancer cells alters the cancer cell cycle and reduces cell division, and found that let-7 is involved in the regulation of cell proliferation; let-7 also has a certain regulatory effect on organs such as the heart [26], bone and muscle [27]. let-7i belongs to the let-7 family, and it has been found that let-7i is found in gastric cancer tissues. The expression is low and may be directly related to coronary heart disease [28]. let-7i may have a regulatory effect on the function of dendritic cells and subpopulations, Let-7 family, a central regulator of energy involved in the regulation of glucose metabolisms [29], has increased expression in HFD rats [30]; secondly, circFUT10 was found to inhibit bovine adipocyte differentiation via let-7 [20]. However, further studies are needed in this study on how bta-let-7i acts. DSCC1, together with chromosome transfer fidelity factors (CHTF) 8 and 18, forms CHTF18-replication factor C, which is involved in the DNA replication process during the S phase of the cell cycle [31,32,33,34,35]. Little is known about DSCC1, and some studies have found that DSCC1 expression may be associated with lung adenocarcinoma [36]; DSCC1 promotes breast cancer by reg-

ulating Wnt/β-catenin signaling and p53 [37]; and colon carcinogenesis is also associated with DSCC1. All of the above studies suggest that DSCC1 expression is associated with cancer production and development, but the role of DSCC1 in the regulation of fat deposition in yak has not been elucidated. 6-phosphofructo-2-kinase/fructose-2,6-bisphosphatases (PFKFB) is a bifunctional enzyme with kinase activity that shunts glucose to the glycolytic pathway and phosphatase activity that shunts glucose to the pentose phosphate pathway [38]. PFKFB consists of four isoforms, PFKFB1, PFKFB2, PFKFB3, and PFKFB4, and each isoform has different functions due to its different kinase-to-phosphatase activity ratios [39]. PFKFB3 plays an important role in glycolytic fluxes due to the highest kinase-to-phosphatase activity ratio [40] and affects the regulation of the cell cycle in the nucleus [41]. However, whether other isoforms are involved in the regulation of fat deposition in yak has not been reported.

In this study, 352 differential circRNAs, 86 differential miRNAs and 3981 differential mRNAs were identified by whole transcriptome sequencing of intramuscular fat in yaks of different months of age. miRNAs and mRNAs network regulation maps were successfully constructed by gene expression correlation analysis and target gene prediction, but the circRNA binding sites have not yet been found on miRNA binding sites on miRNAs. Taking the intersection of the predicted circRNA target genes with the differential miRNAs of intramuscular fat in yaks of different months of age, we obtained two candidate circRNA-miRNA-mRNA pairs that might be related to intramuscular fat deposition in yaks, and found that bta-let-7i might be related to fat deposition in yaks, and might be regulated by X_85287959_85291068. X_85287959_85291068 might be involved in the regulation of intramuscular fat deposition in yak and could be a candidate circRNA to enhance the quality of yak meat. This result could provide a reference for further investigation of the regulatory network of intramuscular fat deposition in yak.

Ethical approval (animals)

The animal handling procedures in this study were approved by the Ethics Committee for the Use of Laboratory Animals, College of Animal Husbandry and Veterinary Science, Qinghai University (Permit No.2023-QHMKY-001).

Financial support

This study was supported by the National Natural Science Foundation of China under Grant No. 32060750, the Qinghai Provincial Science and Technology Program under Grant No. 2024-NK-P41 and 2024-NK-109, and the "Kunlun Talents - High-end Innovative and Entrepreneurial Talents" Project of Qinghai Province.

Declaration of competing interest

The authors declared that they had no conflict of interest.

Acknowledgments

Thank you to all the members of the group.

Supplementary material

https://doi.org/10.1016/j.ejbt.2024.10.004.

Data availability

The authors do not have permission to share data.

References

[1] Wiener G, Han JL, Long RJ. The Yak 2nd edition. Regional Office for Asia and the Pacific Food and Agriculture Organization of the United Nations, Bangkok; 2003.
[2] McCarthy SN, Henchion M, White A, et al. Evaluation of beef eating quality by Irish consumers. Meat Sci 2017;132:118–24. https://doi.org/10.1016/j.meatsci.2017.05.005. PMid: 28522169.
[3] Hunt MR, Legako JF, Dinh TT, et al. Assessment of volatile compounds, neutral and polar lipid fatty acids of four beef muscles from USDA Choice and Select graded carcasses and their relationships with consumer palatability scores and intramuscular fat content. Meat Sci 2016;116:91–101. https://doi.org/10.1016/j.meatsci.2016.02.010. PMid: 26874592.
[4] Piao MY, Baik M. Seasonal variation in carcass characteristics of Korean cattle steers. Asian Australas J Anim Sci 2015;28(3):442–50. https://doi.org/10.5713/ajas.14.0650. PMid: 25656196.
[5] Xiong L, Pei J, Chu M, et al. Fat deposition in the muscle of female and male yak and the correlation of yak meat quality with fat. Animals 2021;11(7):2142. https://doi.org/10.3390/ani11072142. PMid: 34359275.
[6] Luo J, Huang Z, Liu H, et al. Yak milk fat globules from the Qinghai-Tibetan Plateau: Membrane lipid composition and morphological properties. Food Chem 2018;245:731–7. https://doi.org/10.1016/j.foodchem.2017.12.001. PMid: 29287434.
[7] Khan R, Raza SHA, Junjvlieke Z, et al. RNA-seq reveal role of bovine *TORC2* in the regulation of adipogenesis. Arch Biochem Biophys 2020;680, 108236. https://doi.org/10.1016/j.abb.2019.108236. PMid: 31893525.
[8] Du J, Zhang P, Gan M, et al. MicroRNA-204-5p regulates 3T3-L1 preadipocyte proliferation, apoptosis and differentiation. Gene 2018;668:1–7. https://doi.org/10.1016/j.gene.2018.05.036. PMid: 29775748.
[9] Barrett SP, Salzman J. Circular RNAs: Analysis, expression and potential functions. Development 2016;143(11):1838–47. https://doi.org/10.1242/dev.128074. PMid: 27246710.
[10] Huang A, Zheng H, Wu Z, et al. Circular RNA-protein interactions: Functions, mechanisms, and identification. Theranostics 2020;10(8):3503–17. https://doi.org/10.7150/thno.42174. PMid: 32206104.
[11] Abe N, Hiroshima M, Maruyama H, et al. Rolling circle amplification in a prokaryotic translation system using small circular RNA. Angew Chem Int Ed 2013;52(27):7004–8. https://doi.org/10.1002/anie.201302044. PMid: 23716491.
[12] Xu X, Zhang J, Tian Y, et al. CircRNA inhibits DNA damage repair by interacting with host gene. Mol Cancer 2020;19(1):128. https://doi.org/10.1186/s12943-020-01246-x. PMid: 32838810.
[13] Zang J, Lu D, Xu A. The interaction of circRNAs and RNA binding proteins: An important part of circRNA maintenance and function. J Neurosci Res 2020;98(1):87–97. https://doi.org/10.1002/jnr.24356. PMid: 30575990.
[14] Zhou WY, Cai ZR, Liu J, et al. Circular RNA: Metabolism, functions and interactions with proteins. Mol Cancer 2020;19(1):172. https://doi.org/10.1186/s12943-020-01286-3. PMid: 33317550.
[15] Thomas LF, Sætrom P. Circular RNAs are depleted of polymorphisms at microRNA binding sites. Bioinformatics 2014;30(16):2243–6. https://doi.org/10.1093/bioinformatics/btu257. PMid: 24764460.
[16] Chen G, Wang Q, Li Z, et al. Circular RNA CDR1as promotes adipogenic and suppresses osteogenic differentiation of BMSCs in steroid-induced osteonecrosis of the femoral head. Bone 2020;133, 115258. https://doi.org/10.1016/j.bone.2020.115258. PMid: 32018039.
[17] Feng X, Zhao J, Li F, et al. Weighted gene co-expression network analysis revealed that CircMARK3 is a potential CircRNA affects fat deposition in buffalo. Front Vet Sci 2022;9, 946447. https://doi.org/10.3389/fvets.2022.946447. PMid: 35873681.
[18] Zhu Y, Gui W, Lin X, et al. Knock-down of circular RNA H19 induces human adipose-derived stem cells adipogenic differentiation via a mechanism involving the polypyrimidine tract-binding protein 1. Exp Cell Res 2020;387(2), 111753. https://doi.org/10.1016/j.yexcr.2019.111753. PMid: 31837293.
[19] Li H, Yang J, Wei X, et al. CircFUT10 reduces proliferation and facilitates differentiation of myoblasts by sponging miR-133a. J Cell Physiol 2018;233(6):4643–51. https://doi.org/10.1002/jcp.26230. PMid: 29044517.
[20] Jiang R, Li H, Yang J, et al. circRNA profiling reveals an abundant circFUT10 that promotes adipocyte proliferation and inhibits adipocyte differentiation via sponging let-7. Mol Ther Nucleic Acids 2020;20:491–501. https://doi.org/10.1016/j.omtn.2020.03.011. PMid: 32305019.
[21] Wang L, Liang W, Wang S, et al. Circular RNA expression profiling reveals that circ-PLXNA1 functions in duck adipocyte differentiation. PLoS One 2020;15(7), e0236069. https://doi.org/10.1371/journal.pone.0236069. PMid: 32692763.
[22] Li B, He Y, Wu W, et al. Circular RNA profiling identifies novel circPPARA that promotes intramuscular fat deposition in pigs. J Agric Food Chem 2022;70(13):4123–37. https://doi.org/10.1021/acs.jafc.1c07358. PMid: 35324170.
[23] Liu X, Bai Y, Cui R, et al. Sus_circPAPPA2 regulates fat deposition in castrated pigs through the miR-2366/GK pathway. Biomolecules 2022;12(6):753. https://doi.org/10.3390/biom12060753. PMid: 35740877.
[24] Lagos-Quintana M, Rauhut R, Meyer J, et al. New microRNAs from mouse and human. RNA 2003;9(2):175–9. https://doi.org/10.1261/rna.2146903. PMid: 12554859.
[25] Johnson CD, Esquela-Kerscher A, Stefani G, et al. The let-7 microRNA represses cell proliferation pathways in human cells. Cancer Res 2007;67(16):7713–22. https://doi.org/10.1158/0008-5472.CAN-07-1083. PMid: 17699775.

[26] Thum T, Galuppo P, Wolf C, et al. MicroRNAs in the human heart: A clue to fetal gene reprogramming in heart failure. Circulation 2007;116(3):258–67. https://doi.org/10.1161/CIRCULATIONAHA.107.687947. PMid: 17606841.
[27] Harfe BD, McManus MT, Mansfield JH, et al. The RNaseIII enzyme *Dicer* is required for morphogenesis but not patterning of the vertebrate limb. Proc Natl Acad Sci USA 2005;102(31):10898–903. https://doi.org/10.1073/pnas.0504834102. PMid: 16040801.
[28] Satoh M, Tabuchi T, Minami Y, et al. Expression of let-7i is associated with Toll-like receptor 4 signal in coronary artery disease: Effect of statins on let-7i and Toll-like receptor 4 signal. Immunobiology 2012;217(5):533–9. https://doi.org/10.1016/j.imbio.2011.08.005. PMid: 21899916.
[29] Jiang S. A regulator of metabolic reprogramming: MicroRNA Let-7. Transl Oncol 2019;12(7):1005–13. https://doi.org/10.1016/j.tranon.2019.04.013. PMid: 31128429.
[30] Dai LL, Li SD, Ma YC, et al. MicroRNA-30b regulates insulin sensitivity by targeting SERCA2b in non-alcoholic fatty liver disease. Liver Int 2019;39(8):1504–13. https://doi.org/10.1111/liv.14067. PMid: 30721562.
[31] Xue Y, Marvin ME, Ivanova IG, et al. Rif1 and Exo1 regulate the genomic instability following telomere losses. Aging Cell 2016;15(3):553–62. https://doi.org/10.1111/acel.12466. PMid: 27004475.
[32] Keijzers G, Liu D, Rasmussen LJ. Exonuclease 1 and its versatile roles in DNA repair. Crit Rev Biochem Mol Biol 2016;51(6):440–51. https://doi.org/10.1080/10409238.2016.1215407. PMid: 27494243.
[33] Kim JT, Cho HJ, Park SY, et al. DNA replication and sister chromatid cohesion 1 (DSCC1) of the replication factor complex CTF18-RFC is critical for colon cancer cell growth. J Cancer 2019;10(24):6142–53. https://doi.org/10.7150/jca.32339. PMid: 31762824.
[34] Boehm EM, Gildenberg MS, Washington MT. The Many Roles of PCNA in Eukaryotic DNA Replication. In: Kaguni LS, Oliveira MT, editors. The Enzymes. Academic Press; 2016. p. 231–54. https://doi.org/10.1016/bs.enz.2016.03.003. PMid: 27241932.
[35] Bermudez VP, Maniwa Y, Tappin I, et al. The alternative Ctf18-Dcc1-Ctf8-replication factor C complex required for sister chromatid cohesion loads proliferating cell nuclear antigen onto DNA. Proc Natl Acad Sci USA 2003;100(18):10237–42. https://doi.org/10.1073/pnas.1434308100. PMid: 12930902.
[36] Chang S, Zhu Y, Xi Y, et al. High DSCC1 level predicts poor prognosis of lung adenocarcinoma. Int J Gen Med 2021;14:6961–74. https://doi.org/10.2147/IJGM.S329482. PMid: 34707388.
[37] Jin G, Wang W, Cheng P, et al. DNA replication and sister chromatid cohesion 1 promotes breast carcinoma progression by modulating the Wnt/β-catenin signaling and p53 protein. J Biosci 2020;45:127. https://doi.org/10.1007/s12038-020-00100-y. PMid: 33184243.
[38] Bartrons R, Simon-Molas H, Rodríguez-García A, et al. Fructose 2,6-bisphosphate in cancer cell metabolism. Front Oncol 2018;8:331. https://doi.org/10.3389/fonc.2018.00331. PMid: 30234009.
[39] De Bock K, Georgiadou M, Carmeliet P. Role of endothelial cell metabolism in vessel sprouting. Cell Metab 2013;18(5):634–47. https://doi.org/10.1016/j.cmet.2013.08.001. PMid: 23973331.
[40] Li FL, Liu JP, Bao RX, et al. Acetylation accumulates PFKFB3 in cytoplasm to promote glycolysis and protects cells from cisplatin-induced apoptosis. Nat Commun 2018;9(1):508. https://doi.org/10.1038/s41467-018-02950-5. PMid: 29410405.
[41] Yalcin A, Clem BF, Imbert-Fernandez Y, et al. 6-Phosphofructo-2-kinase (PFKFB3) promotes cell cycle progression and suppresses apoptosis via Cdk1-mediated phosphorylation of p27. Cell Death Dis. 2014;5(7):. https://doi.org/10.1038/cddis.2014.292. PMid: 2503286e1337.